Supplementary Table S1. Adenocarcinoma of the lung with EDB expression.

Patient ID	EDB expression	Tumor volume (cm)	Metastasis
202115617B	+	1.0×0.6×0.6	No
202111705B	+	1.1×0.9×0.7	No
202115645D	++	2.1×1.1×0.7	No
202113284F	++	2.8×2.2×1.5	No
202112349E	+++	Lack of data	Lymph node metastases
202115643C	+++	3.2×2.9×2.3	Lymph node metastases

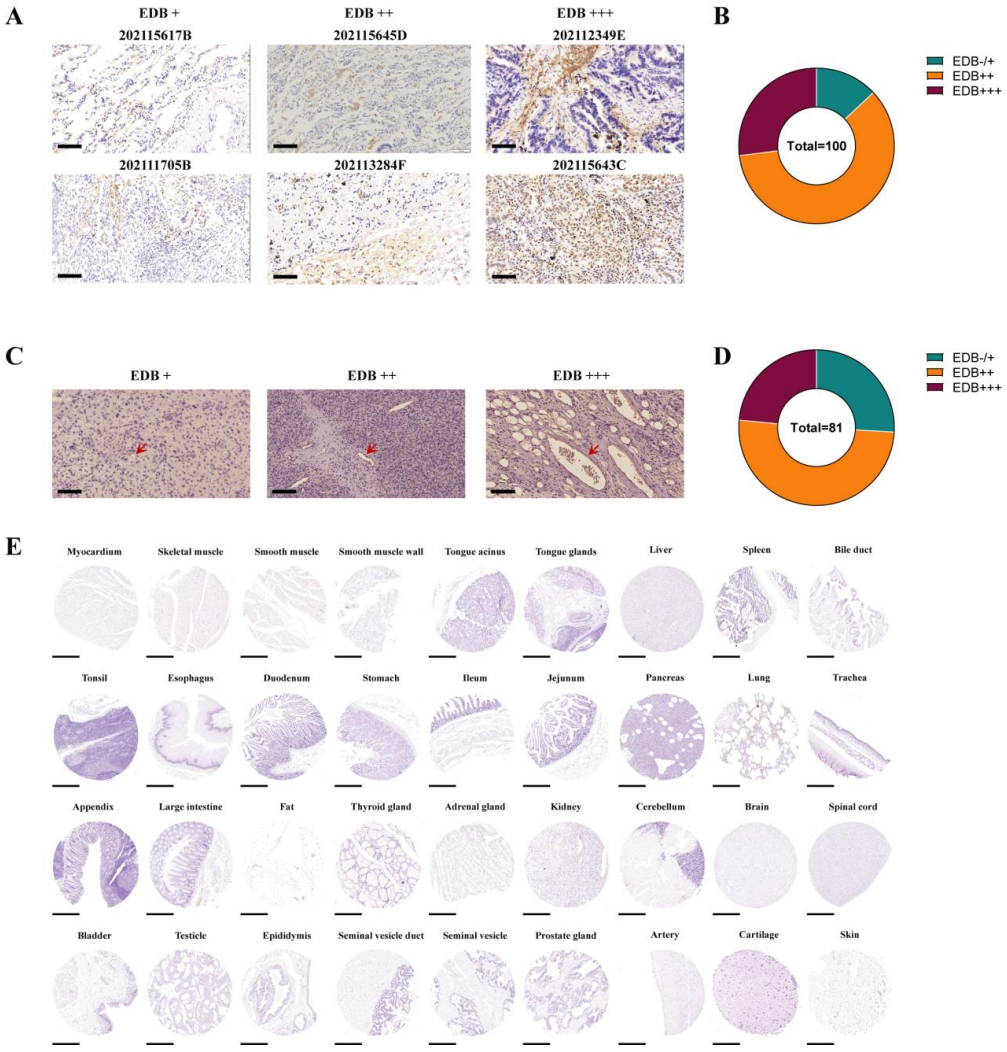

Supplementary Figure S1. Expression of EDB fibronectin detected by IHC using the anti-EDB antibody L19. (A) Representative IHC for lung cancer tissues of different stages of disease. Scale bar: 100 μm. **(B)** EDB fibronectin expression levels of 100 different lung carcinoma samples were rated. **(C)** Representative IHC staining from the K105Sf01 microarray (bioaitech). Scale bar: 100 μm. **(D)** EDB fibronectin expression levels of 81 sarcoma samples were rated. **(E)** IHC failed to detect any EDB fibronectin expression in 120 normal human tissues in a microarray (HOrgN120PT01, Outdo Biotech)

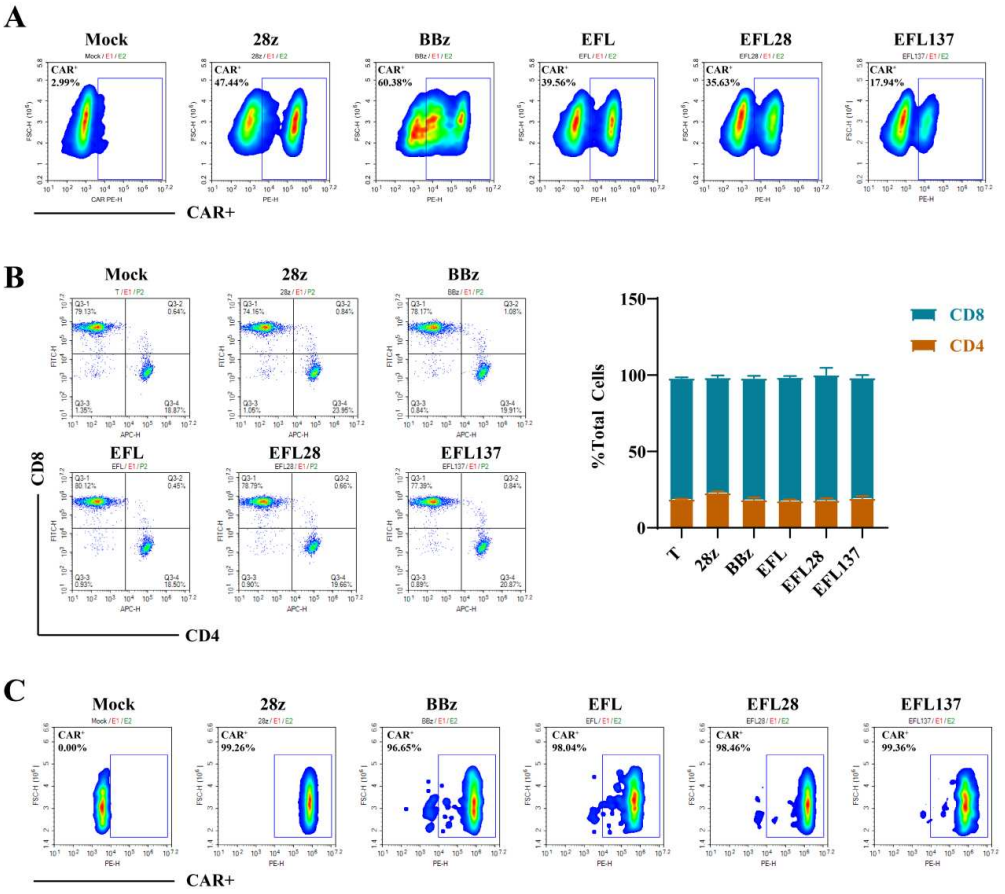

Supplementary Figure S2. Expression of CAR receptor on T cells. (A) T cells were isolated from six donors and transduced with lentiviral vectors carrying chimeric receptor genes. Representative flow cytometry data for one donor show cell surface expression of EDB-targeting 2nd G CARs or TCR-CARs on primary human T cells. **(B)** Flow cytometric detection of CD4 and CD8 subsets of purified CAR-T cells for one donor. **(C)** Characterization of CAR-positive Jurkat cells purified by anti-scFv antibody and magnetic beads.

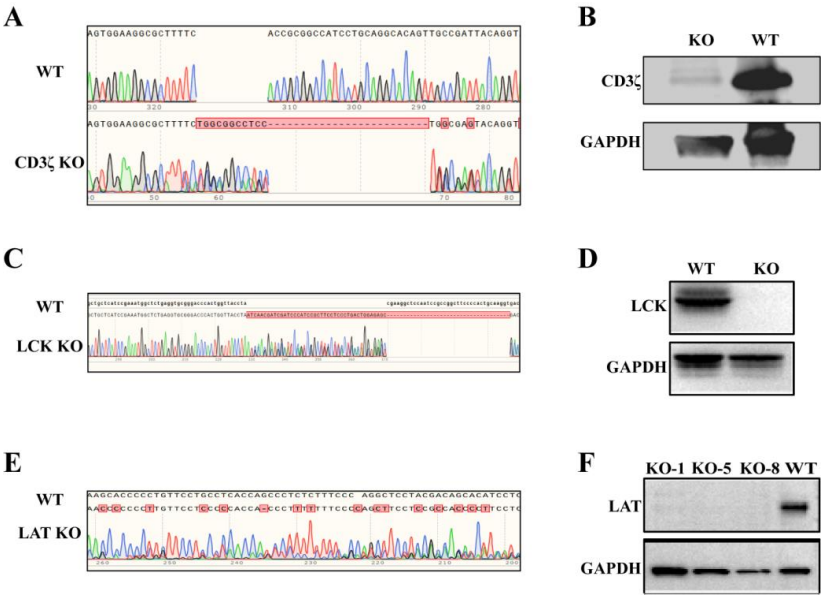

Supplementary Figure S3. Knockout of CD3ζ, LCK, or LAT genes in Jurkat cells by CRISPR Cas9. (A) Wild-type and **(B)** Jurkat^{CD3ζKO} cell lines were analyzed by Sanger sequencing and Western blotting. **(C)** Wild-type and **(D)** Jurkat$^{LAT\ KO}$ cell lines were detected by Sanger sequencing and Western blotting. **(E)** Wild-type and **(F)** Jurkat$^{LCK\ KO}$ cell lines were detected by Sanger sequencing and Western blot.

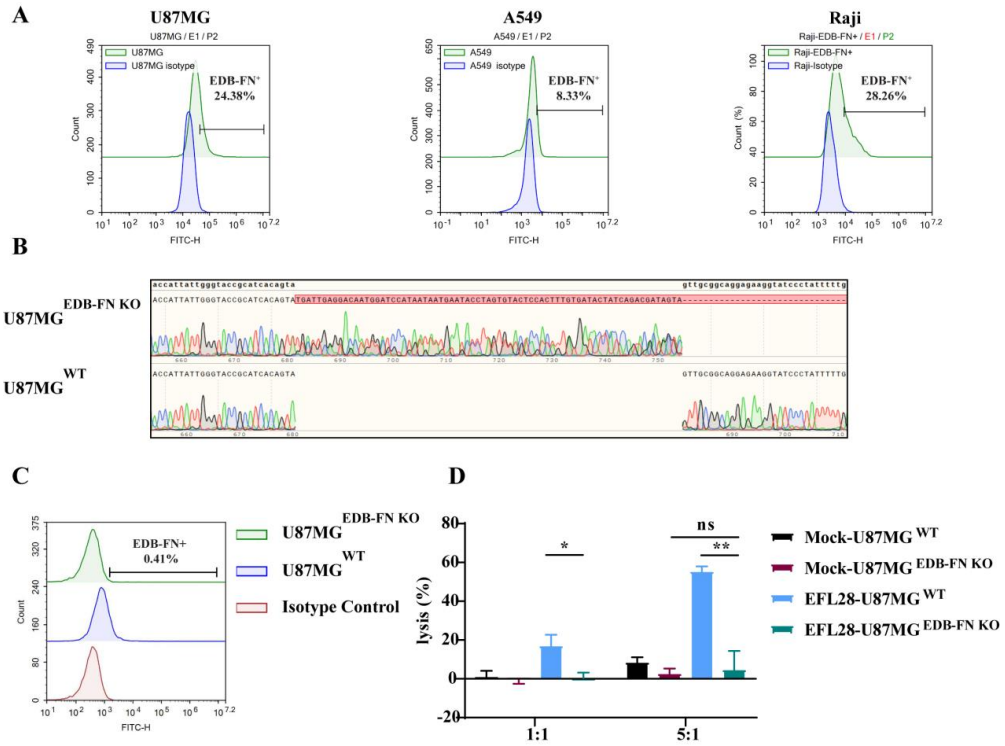

Supplementary Figure S4. EDB-targeting EFL28 TCR-CAR T cells exhibit antigen-dependent cytotoxicity. **(A)** The expression of EDB in U87MG, A549, and Raji cells was detected by flow cytometry. No expression of EDB in MCF-7 cells was found by Western blotting and qPCR (not shown). **(B)** and **(C)** U87MG$^{EDB\ KO}$ cell lines were detected by Sanger sequencing and Western blotting. **(D)** Effector cells were cocultured with U87MG^{WT} or U87MG$^{EDB\ KO}$ cells for 24 h according to the effect-to-target ratio = 5:1, and LDH in the supernatant was detected. Statistical significance was calculated by one-way analysis of variance (ANOVA) with Bonferroni post hoc test, n =3, *P<0.05, **P<0.01.

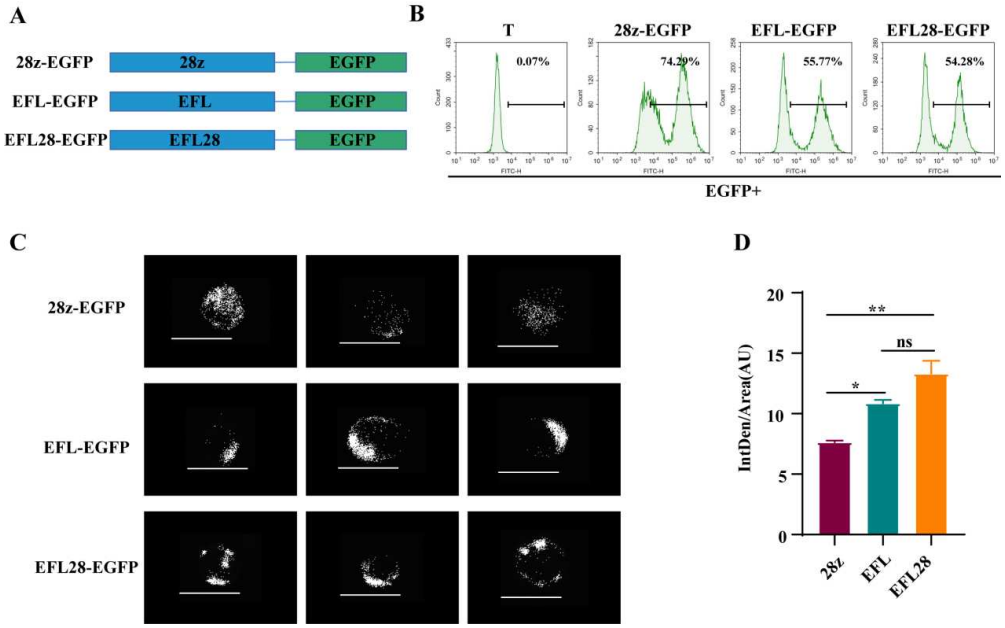

Supplementary Figure S5. EFL28 receptor binding to antigen mediates immune synapse formation. (A) Schematic representation of chimeric receptors. **(B)** Representative flow cytometry data for surface expression of EDB-targeting 2nd G CARs or TCR-CARs on primary human T cells. **(C)** Sequestering of 2nd G CARs or TCR-CARs upon EDB antigen stimulation was detected by confocal laser microscopy, scale bar =10 μm. **(D)** Average fluorescence intensity of CARs or TCR-CARs, n=3. IntDen (Integrated Density): the sum of fluorescence intensities; Area: fluorescent area. Statistical significance was calculated by two-way analysis of variance (ANOVA) with Bonferroni post hoc test, $^{**}P<0.01$, $^{***}P<0.001$.

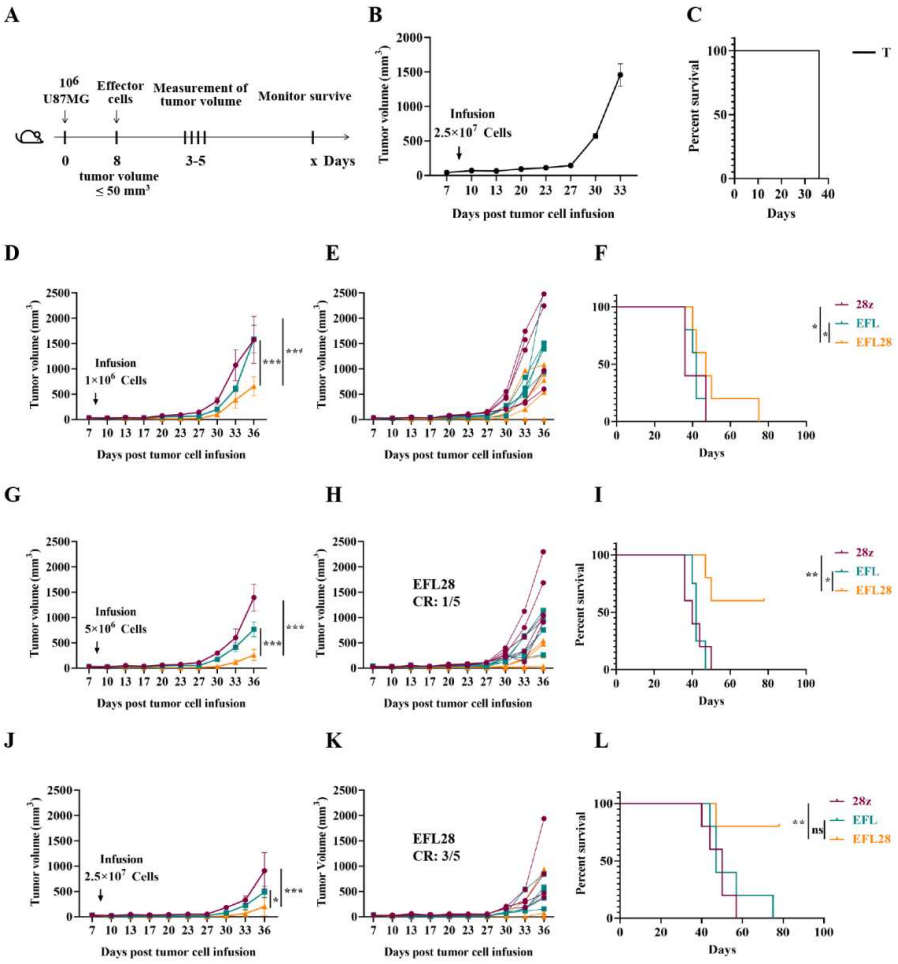

Supplementary Figure S6. Dose-dependent efficacy of anti-EDB TCR-CAR T cells against U87MG tumor in NCG mice. (A) Schematics for the small tumor (tumor size < 50 mm^3) in vivo testing. **(B)** Twenty-five million activated but nontransduced T cells were infused as a model for uncontrolled U87MG tumors, n=3, and **(C)** mice were sacrificed when tumor sizes exceeded 2000 mm^3 at approximately 36 days after implantation. **(D-L)** Three different doses of CAR T cells as indicated were infused when tumor volumes were less than 50 mm^3, and mice were monitored for up to 100 days. Average tumor growth, tumor growth of individual mice, and overall survival curve are shown for $1x10^6$ CAR T cells **(D, E, F)**, for $5x10^6$ CAR T cells **(G, H, I)**, or for $2.5x10^7$ CAR T cells **(J, K, L)**; n=5 for each CAR/dose group. Statistical significance for the difference

was analyzed by two-way analysis of variance (ANOVA) with Bonferroni post hoc test. Survival was plotted using a Kaplan−Meier curve, and statistically significant differences were analyzed using the log-rank test, $^{*}P<0.05$, $^{**}P<0.01$, $^{***}P<0.001$.

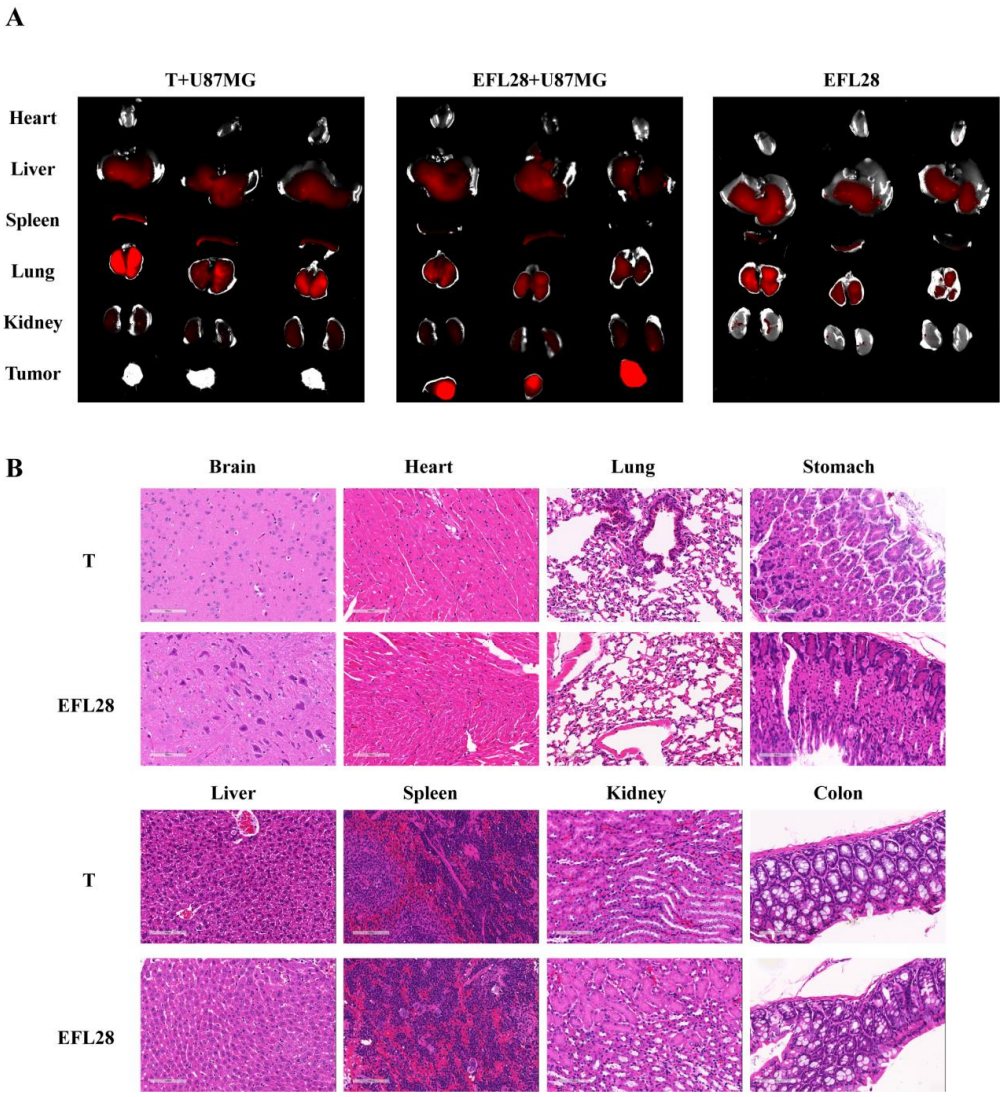

Supplementary Figure S7. The on-target off-tumor effect of EFL28 TCR-CAR T cells. (A) 10^7 T cells or EFL28 TCR-CAR T cells labeled with red fluorescence were injected into the tail vein of U87MG tumor-bearing NCG mice (left and middle), and EFL TCR-CAR T cells were also injected into nontumorous NCG mice (right). Fluorescence imaging of organs was taken 48 hours later, n=3. **(B)** 10^7 T or EFL28 TCR-CAR T cells were injected into the tail vein of U87MG tumor-bearing mice, and the organs were harvested for hematoxylin-eosin staining 14 days later, n=3.

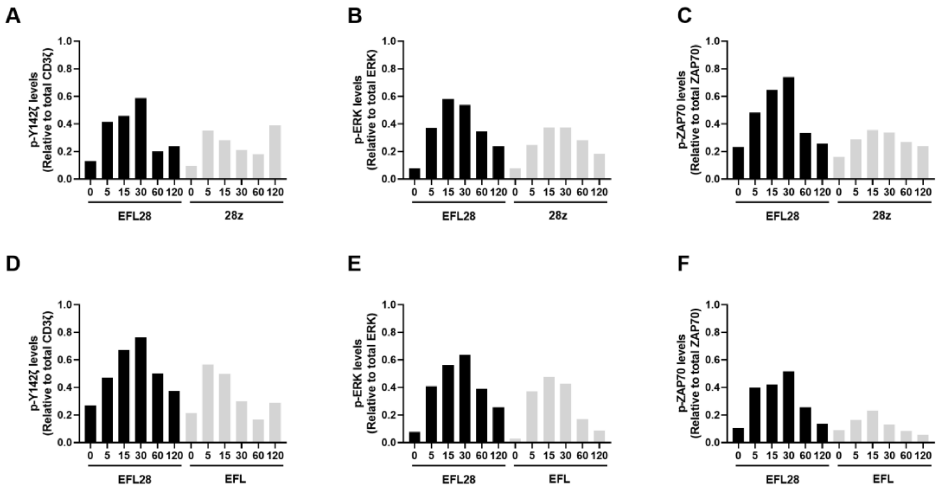

Supplementary Figure S8. Optical density analysis for phosphorylated protein levels relative to the total protein based on Western Blot of Figure 6A. (A), **(B)**, **and (C)** Analysis of phosphorylated protein levels of CD3ζ, ERK, and ZAP70 in EFL28 and 28ζ receptor-mediated T cells after antigen stimulation**,** Figure 6A left panel. **(D)**, **(E)**, **and (F)** Analysis of phosphorylated protein levels of CD3ζ, ERK, and ZAP70 in EFL28 and EFL receptor-mediated T cells after antigen stimulation**,** Figure 6A right panel.

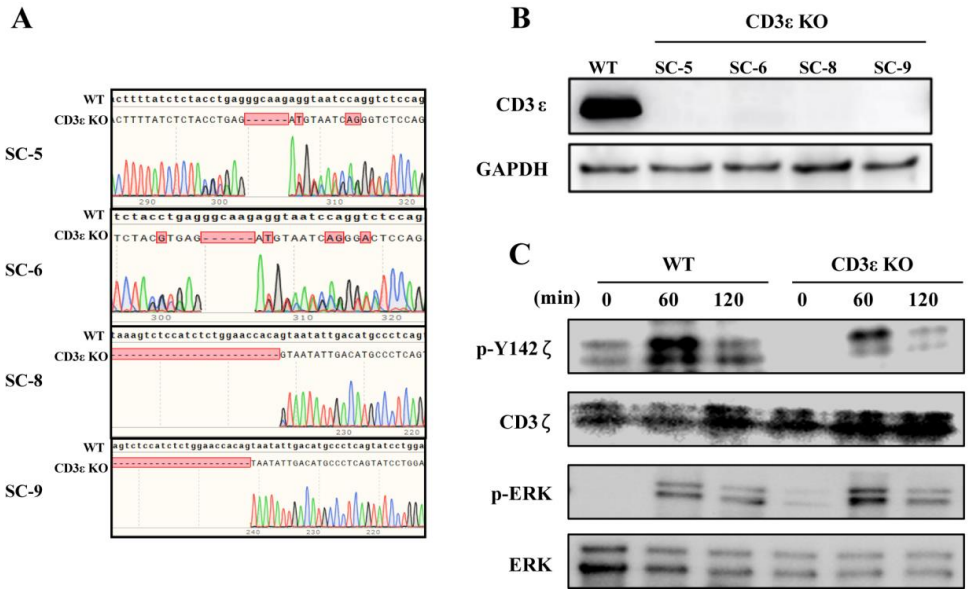

Supplementary Figure S9. EFL28 receptor signal via CD3ζ. (A) and **(B)** Jurkat$^{CD3\varepsilon\ KO}$ cell lines were detected by Sanger sequencing and Western blot. **(C)** Wild-type Jurkat cells or Jurkat$^{CD3\varepsilon\ KO}$ cells were transduced with lentivirus to express the EFL28 receptor. The effector cells were co-incubated with 5 μg/ml EDB protein, and lysis buffer was added at the specified time to terminate the reaction. The phosphorylation levels of CD3ζ and ERK in whole-cell lysates were detected by Western blot.

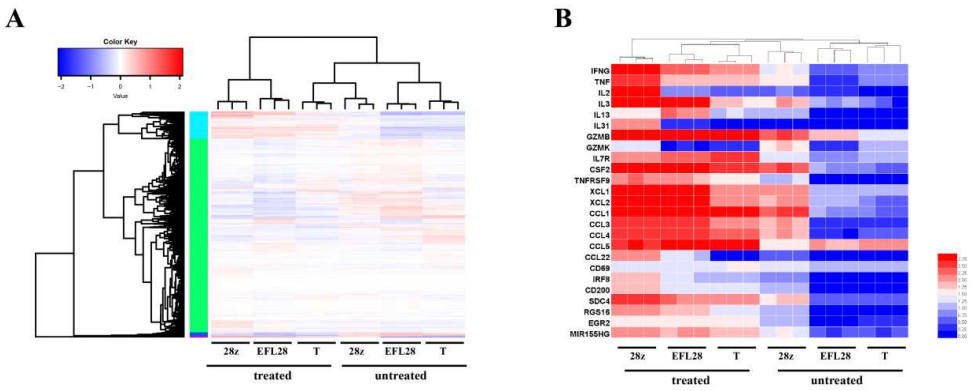

Supplementary Figure S10. Hierarchical clustering analysis of differentially expressed genes.

(A) 28z CAR-T cells and EFL28 TCR-CAR T cells were divided into 2 aliquots. One aliquot was exposed to U87MG at an effect-to-target ratio of 5:1 for 24 hours, and the other aliquot was left untreated. Similarly, the T-cell aliquot was stimulated by adding CD3/CD28 antibody-coupled magnetic beads for 24 hours or was left untreated. RNA was extracted and sequenced. n=3. **(B)** Expression changes for select gene list associated with T cell activation.